Supplementary Material to

Anthropogenic-biogenic interactions and regional transport drive summer ozone formation in an agricultural-urban interface of Northeast China

Xinpeng Ye[1, a], Qian Jiang[2, 3, a], Jin Ban[1], Mengyu Xie[4], Qianyi Xu[1], Zeyu Wang[1], Jian Sun[1*], Hongai Zhang[5], Xinyi Niu[6], Hongmei Xu[1], Zhenxing Shen[1], Guohui Li[3]

[1]*Department of Environmental Science and Engineering, Xi'an Jiaotong University, Xi'an 710049, China*

[2]*School of Environmental Science and Engineering, Southwest Jiaotong University, Chengdu, 611756, Sichuan, China.*

[3]*Key Lab of Aerosol Chemistry & Physics, SKLLQG, Institute of Earth Environment, Chinese Academy of Sciences, Xi'an 710049, China*

[4]*East China University of Science and Technology, Shanghai 200237, China*

[5]*Department of Neonatology, Shanghai General Hospital Affiliated to Shanghai Jiao Tong University School of Medicine, 650 Xinsongjiang Rd, Songjiang District, Shanghai 201620, China*

[6]*Department of Occupational and Environmental Health, School of Public Health, Xi'an Jiaotong University Health Science Center, Xi'an 710049, China*

**Author to whom correspondence should be addressed. E-mail: sunjian0306@mail.xjtu.edu.cn (Jian Sun).*

Captions:

Text S1. VOC analysis

Text S2. WRF-Chem model parameter settings

Text S3. Factor separation approach (FSA)

Text S4. PMF source apportionment of VOCs in Siping

Fig. S1 Location of the Yishangchang National Air Quality Monitoring Station in Siping (Ye et al., 2025)

Fig. S2 Topography and spatial distribution of (a) the WRF-Chem modeling domain and (b) the research area, the thin black solid lines denote the boundary of Jilin Province, while the thick black solid lines indicate the administrative boundary of Siping.

Fig. S3 Time series of observed (black dots) and simulated (red lines) hourly O_3 concentrations at the national air quality monitoring stations in Jilin Province and Siping from 11 to 18 June 2021.

Fig. S4 Spatial distributions of observed (colored circles) and simulated (colored shading) concentrations of (a) $PM_{2.5}$, (b) MDA8 O_3, (c) NO_2, and (d) SO_2 at the national air quality monitoring stations during 11-18 June 2021.

Fig. S5 Spatial distributions of background MDA8 O_3 concentrations and the mean contributions of local emissions and regional transport to MDA8 O_3 concentrations in Siping and surrounding areas during 11-18 June 2021.

Fig. S6 Spatial distributions of the percentage contributions of industrial, power plant, residential, transportation, agricultural and biogenic sources to MDA8 O_3 concentrations in Siping during 11-18 June 2021.

Table S1. VOC species measured in Siping.

Table S2. WRF-Chem model settings

Table S3. Sensitivity experiment design for quantifying the contributions of local emissions and regional transport to O_3.

Table S4. Sensitivity experiment design for major emission sources affecting O_3.

Table S5. Mean concentrations and chemical composition of ambient VOCs in Siping during 2021-2022.

Table S6. Concentration characteristics of ambient VOC species in Siping during 2021-2022.

Table S7. Top 15 VOC species in ambient air in Siping during 2021-2022 (ppbv).

Table S8. Top 10 VOC species contributing to OFP by month in Siping during 2021-2022.

Table S9. Top 10 VOC species contributing to OFP during the morning, afternoon, and

56 evening in Siping during 2021-2022.

57 **Table S10.** Contributions of local emissions and regional transport to MDA8 O_3
58 concentrations in Siping during the simulation period.

59 **Table S11.** Emission reduction scenarios for transportation and industrial sources in
60 Siping.

Text S1. VOC analysis

The analysis of VOCs followed the methods specified in the Chinese standards Ambient Air-Determination of Volatile Organic Compounds-Canister Sampling/Gas Chromatography-Mass Spectrometry (HJ 759-2015), 2019 Ambient Air VOC Monitoring Program for Prefecture-Level and Above Cities (Monitoring Letter [2019] No. 11), Technical Guidelines for Ambient Volatile Organic Compound (VOC) Monitoring in Urban Areas (Trial Version, Draft for Comments), and the U.S. EPA Method TO-14 (Determination of Volatile Organic Compounds (VOCs) in Ambient Air Using Specially Prepared Canisters With Subsequent Analysis by Gas Chromatography). A cryogenic preconcentration system (Entech 7200, Entech Instruments Inc., USA) coupled with a gas chromatography-mass spectrometry system (7890B GC/5977B MSD, Agilent Technologies, USA) was used to qualitatively and quantitatively determine 106 VOC species, including alkanes, alkenes, alkynes, aromatic hydrocarbons, halocarbons, and oxygenated volatile organic compounds (OVOCs).

The baseline period of this study covered 2021-2022, with VOC sampling conducted during July and August, when O_3 pollution is most severe. Ambient VOC samples were collected using 3.2 L SUMMA canisters with specially passivated inner surfaces and 3 h integrated samplers. Before sampling, all SUMMA canisters were thoroughly cleaned and evacuated. The integrated samplers were equipped with calibrated flow restrictors to maintain a constant sampling flow rate throughout the 3 h collection period, ensuring representative air samples. During sampling, the SUMMA canisters were connected to the integrated samplers, and ambient air was drawn into the canisters by the pressure difference between the inside and outside of the canister and subsequently stored for analysis.

Qualitative and quantitative analyses of the target compounds were performed using calibration curves established with certified standard gas mixtures. Compound identification was based on chromatographic retention times and mass spectra, whereas quantification was conducted using the internal standard method by comparing the chromatographic peak areas of the samples with those of the calibration standards. Low-concentration calibration curves were used for ambient air samples, whereas high-concentration calibration curves were applied to source samples. For the low-concentration calibration, the U.S. EPA Photochemical Assessment Monitoring Stations (PAMS) standard mixture (57 non-methane hydrocarbons, 1 ppmv), the TO-15 standard

mixture (64 VOC species; Spectra Gases, USA), and a mixed standard containing 13 aldehydes and ketones were diluted using a high-precision dilution system (Entech 4700) to generate secondary standards at 1, 2, 5, and 10 ppbv. For the high-concentration calibration, the same standards were diluted to 5, 10, 20, and 30 ppbv. Calibration standards and one zero-air sample were analyzed using the same analytical procedure as that used for field samples. Calibration curves were established for each target compound, and all correlation coefficients (R^2) exceeded 0.99.

For VOC samples collected from representative emission sources, concentrations varied over a wide range. To ensure that detector responses remained within the linear calibration range, each sample was first subjected to a preliminary analysis. Based on the preliminary results, an appropriate dilution factor was determined. The sample was then diluted with high-purity nitrogen using the high-precision dilution system and reanalyzed. Final compound identification and quantification were performed according to chromatographic retention times and detector responses.

Text S2. WRF-Chem model parameter settings

In this study, the optimized WRF-Chem model (Li et al., 2016) was used to analyze the formation and sources of $PM_{2.5}$ in Siping City during the study period. When simulating with the WRF-Chem model, multiple parameters were considered, including the terrain, altitude, climate characteristics, weather conditions, and actual atmospheric conditions of the target study area. Several physical process parameterization schemes were set during the simulation process, including: the Morrison cloud microphysics scheme (Morrison et al., 2009), the Grell-3 cumulus parameterization scheme (Grell et al., 2005), the Mellor-Yamada-Janjie (MYJ) boundary layer scheme (Mellor and Yamada, 1982; Janjić, 1990), the Eta surface parameterization scheme based on the Monin and Obukhov (1954)similarity theory, the Noah land surface process scheme (Chen and Dudhia, 2001), and the Goddard longwave and shortwave radiation schemes(Chou and Suarez, 1994).

The chemical mechanism from the US Environmental Protection Agency (US EPA) was coupled into the WRF-Chem model using the CMAQ aerosol mechanism (version 4.6), and corresponding optimizations were made to accurately simulate the dynamic processes of aerosols in the atmosphere (Binkowski and Roselle, 2003). Meanwhile, the WRF-Dust module was incorporated into the WRF-Chem model to simulate the emissions, transport, and deposition of dust. The WRF-Dust module includes five different particle size bins with effective diameters of 1.4, 2.8, 4.8, 9.0, and 16.0 μm. The module includes processes of emission, transport, and both wet and dry deposition (Ginoux et al., 2001).

Text S3. Factor separation approach (FSA)

Chemical transport models are widely used to quantify the contributions of different factors to atmospheric pollutant formation and to support the development of emission control strategies. However, because atmospheric chemistry is inherently nonlinear, the influence of an individual factor cannot be evaluated directly. The total effect of a given factor can be decomposed into its direct contribution and its interaction with other factors. The FSA is a widely adopted method for quantifying both the individual contributions of different factors and their nonlinear interactions.

As an illustrative example, consider two interacting factors, X and Y, that jointly influence pollutant formation. Let f_{XY}, f_X, f_Y, and f_0 denote the model simulations that include both factors, only factor X, only factor Y, and neither factor, respectively. The direct contributions of factors X and Y（f_X' and f_Y'）are calculated as follows:

$$f_X' = f_X - f_0$$

$$f_Y' = f_Y - f_0$$

The simulation including both factors can be expressed as:

$$f_{XY} = f_0 + f_X' + f_Y' + f_{XY}'$$

Where f_{XY}' represents the interaction term between factors X and Y. Accordingly, the interaction effect is calculated as:

$$f_{XY}' = f_{XY} - f_0 - f_X' - f_Y' = f_{XY} - (f_X - f_0) - (f_Y - f_0) - f_0 = f_{XY} - f_X - f_Y + f_0$$

Therefore, quantifying the interaction between factors X and Y requires four model simulations: f_{XY}, f_X, f_Y, 和f_0. This framework enables the nonlinear effects of multiple driving factors on atmospheric pollutant formation to be explicitly separated into their individual and interaction components.

Text S4. PMF source apportionment of VOCs in Siping

Based on the PMF results, VOC emissions in Siping were classified into five major source categories: vehicle emission, industrial combustion, solvent source, gaseous fuel, and biogenic source.

Factor 1 was characterized by high contributions of aromatic hydrocarbons and several halocarbons, including styrene, ethylbenzene, xylenes, ethyl acetate, and chloroform. In particular, styrene and ethyl acetate exhibited exceptionally high loadings. These compounds are commonly associated with industrial solvent use, such as coating, painting, and polymer manufacturing. Chloroform is also a typical industrial solvent (Sha et al., 2021; Wang et al., 2023). In addition, pesticide application in Siping reached 3,213.58 t in 2022. A previous study conducted in Changchun, a neighboring city of Siping, reported that VOC emissions from pesticide spraying were dominated by halocarbons (27-44%), OVOCs (25-38%), and aromatic hydrocarbons (15-28%) (Li et al., 2024), which closely matches the chemical profile of this factor. Therefore, Factor 1 was identified as the solvent use source.

Factor 2 was dominated by light hydrocarbons, including ethylene, ethane, and propylene, together with detectable amounts of Freon-11, Freon-12, chloromethane, and methyl tert-butyl ether (MTBE). Light hydrocarbons, particularly short-chain alkanes, are widely recognized as tracers of gaseous fuel use and incomplete combustion, especially emissions from natural gas and liquefied petroleum gas (LPG) (Wu et al., 2023a). Meanwhile, chlorofluorocarbons are commonly emitted from petrochemical activities and refrigeration systems, whereas MTBE is a well-known gasoline additive (Man et al., 2020; Zhu et al., 2025). Collectively, these characteristics indicate a mixed source associated with gaseous fuel use, combustion processes, and refrigerant emissions. Accordingly, Factor 2 was assigned to the gaseous fuel source.

Factor 3 was distinguished by an exceptionally high loading of isoprene, accompanied by abundant OVOCs, including methyl isobutyl ketone, methyl butyl ketone, and isopropanol. Isoprene is a well-established tracer of biogenic emissions and is emitted primarily by vegetation (Vestenius et al., 2021; Wu et al., 2023b). The coexistence of abundant OVOCs suggests the formation of secondary oxidation products through atmospheric photochemical reactions (Wang et al., 2024). Therefore, Factor 3 was interpreted as a combination of biogenic emissions and secondary photochemical production.

Factor 4 exhibited high loadings of C_4-C_6 alkanes and alkenes, including isopentane, n-

pentane, n-butane, and cis-2-butene, together with a substantial contribution from toluene. Isopentane is widely recognized as a key tracer of gasoline-related emissions, particularly fuel evaporation and vehicle exhaust (Zi et al., 2023; Sun et al., 2021). The presence of alkenes, such as ethylene, further indicates incomplete combustion processes associated with combustion sources, petrochemical activities, and vehicular emissions (Man et al., 2020; Zhou et al., 2020). These chemical characteristics are consistent with both exhaust and evaporative emissions from motor vehicles. Therefore, Factor 4 was identified as the vehicle emission source.

Factor 5 was characterized by high abundances of heavier aromatic hydrocarbons, including trimethylbenzene and diethylbenzene, together with long-chain alkanes such as n-decane and n-dodecane. These compounds are typically associated with diesel exhaust, fuel combustion, and lubricant-related emissions. Compared with factors dominated by light VOCs, the predominance of heavier hydrocarbons indicates emissions originating from high-temperature combustion processes and the incomplete combustion of heavy fuels (Liang et al., 2020; Lyu et al., 2021; Frischmon and Hannigan, 2024). Accordingly, Factor 5 was identified as the diesel-related heavy-oil industrial combustion source.

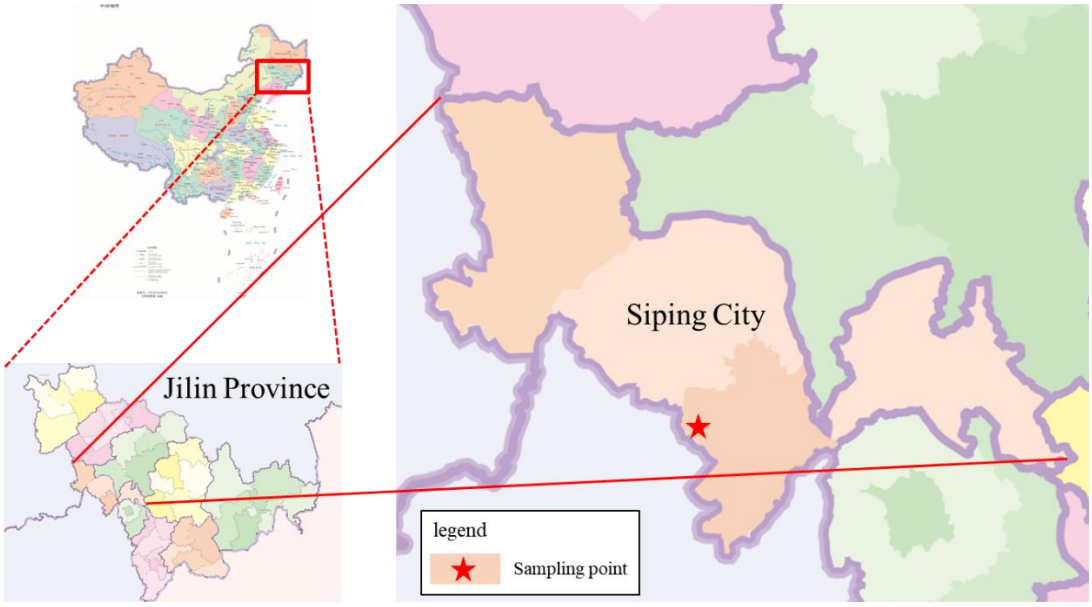

Fig. S1 Location of the Yishangchang National Air Quality Monitoring Station in Siping (Ye et al., 2025)

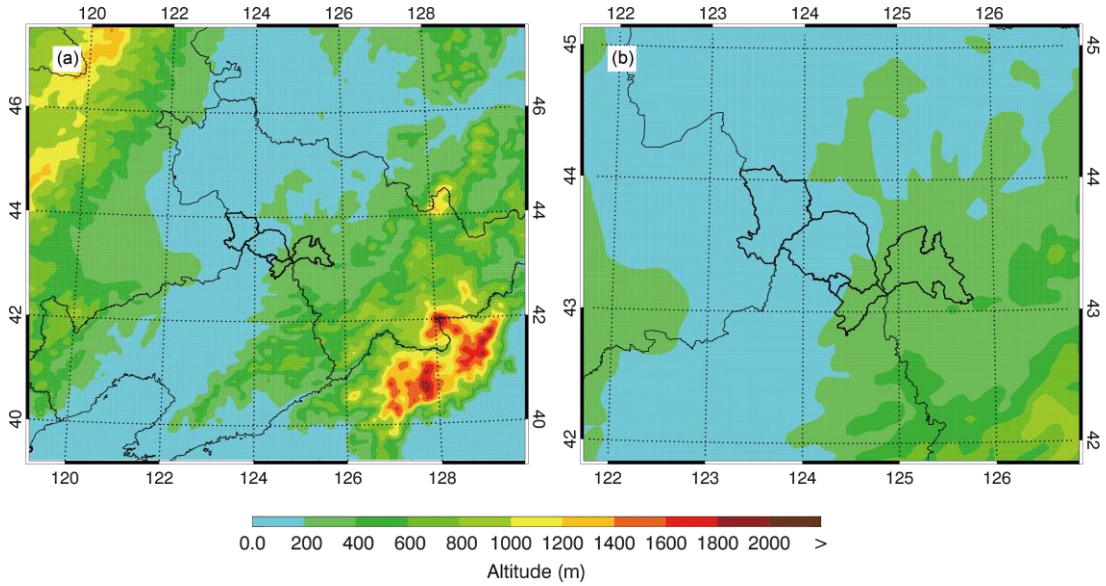

Fig. S2 Topography and spatial distribution of (a) the WRF-Chem modeling domain and (b) the research area, the thin black solid lines denote the boundary of Jilin Province, while the thick black solid lines indicate the administrative boundary of Siping.

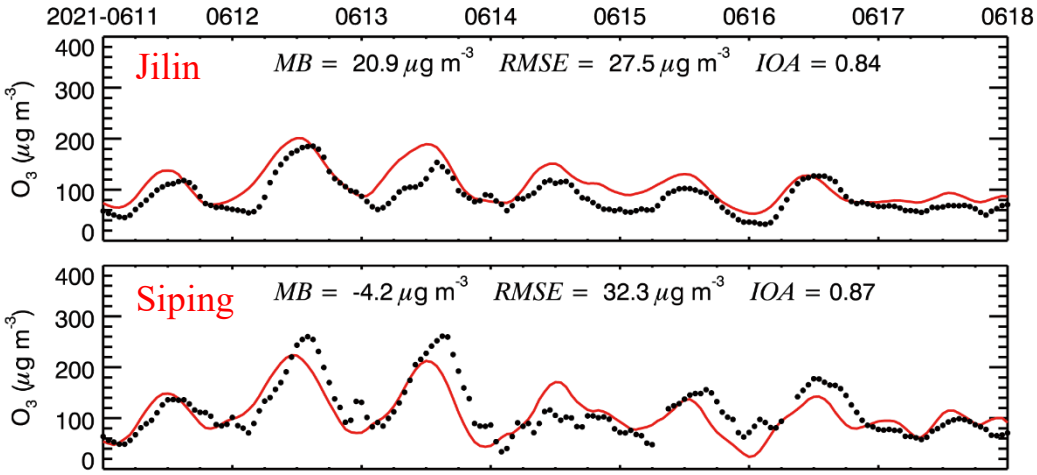

Fig. S3 Time series of observed (black dots) and simulated (red lines) hourly O_3 concentrations at the national air quality monitoring stations in Jilin Province and Siping from 11 to 18 June 2021.

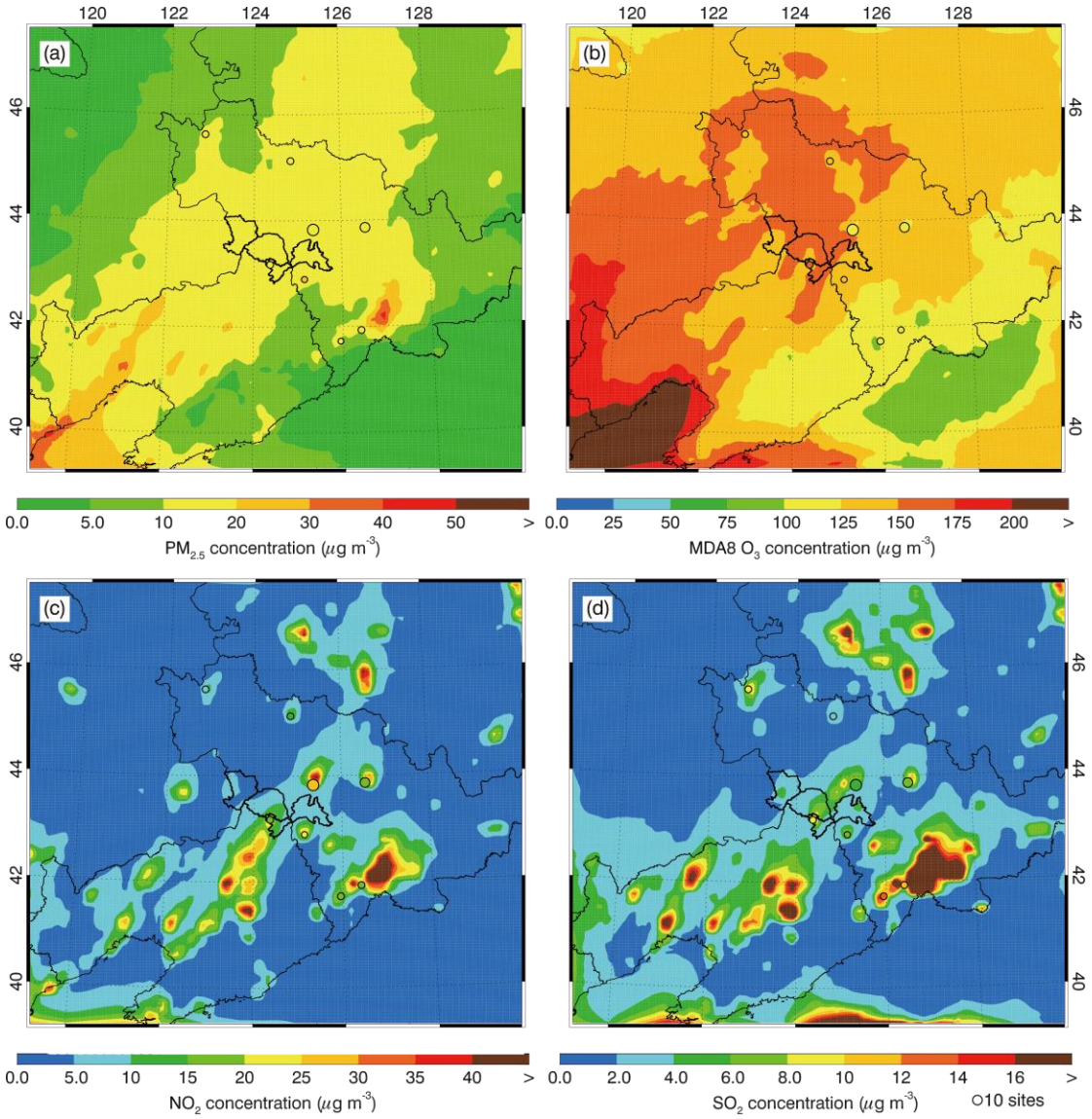

Fig.S4 Spatial distributions of observed (colored circles) and simulated (colored shading) concentrations of (a) $PM_{2.5}$, (b) MDA8 O_3, (c) NO_2, and (d) SO_2 at the national air quality monitoring stations during 11-18 June 2021.

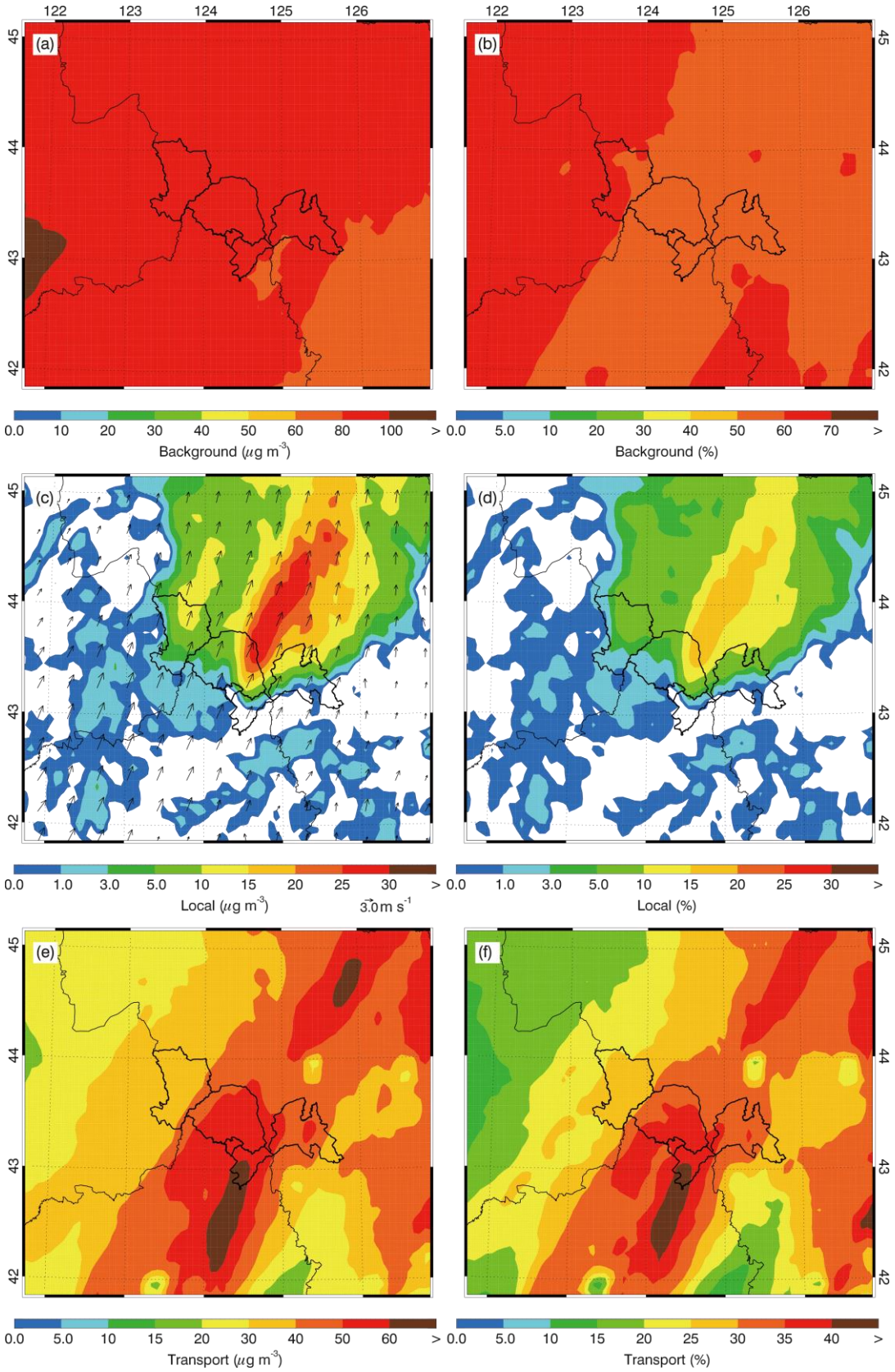

Fig. S5 Spatial distributions of background MDA8 O_3 concentrations and the mean contributions of local emissions and regional transport to MDA8 O_3 concentrations in Siping and surrounding areas during 11-18 June 2021.

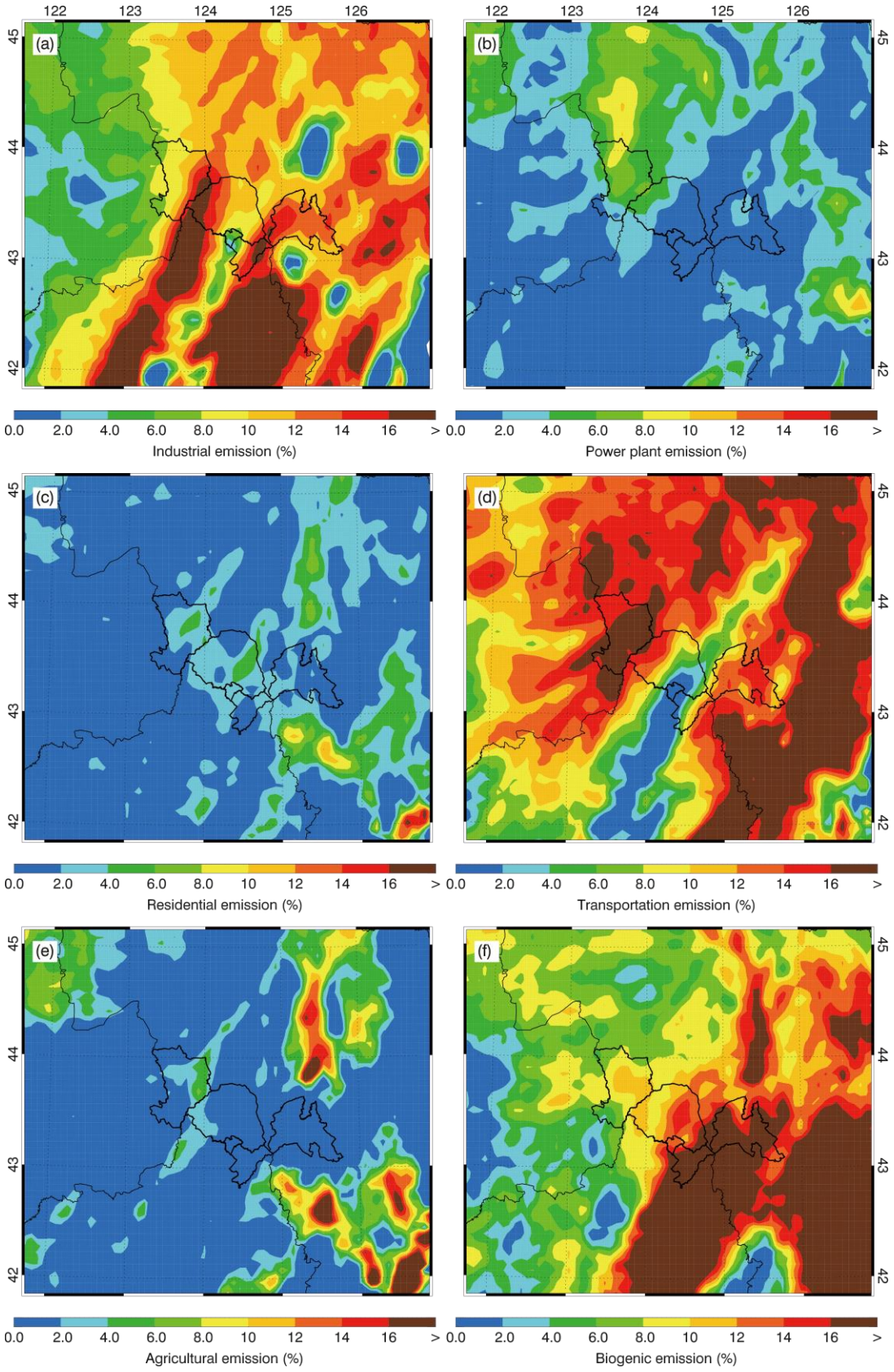

Fig. S6. Spatial distributions of the percentage contributions of industrial, power plant, residential, transportation, agricultural and biogenic sources to MDA8 O_3 concentrations in Siping during 11-18 June 2021.

Table S1. VOC species measured in Siping.

	Compound		Compound
1	Ethylene	54	p-Diethylbenzene
2	Acetylene	55	n-Undecane
3	Ethane	56	n-Dodecane
4	Propylene	57	Freon-12
5	Propane	58	Chloromethane
6	Isobutane	59	Freon-114
7	1-Butene	60	Vinyl-chloride
8	n-Butane	61	1,3-Butadiene
9	Trans-2-butene	62	Bromomethane
10	Cis-2-Butene	63	Chloroethane
11	Isopentane	64	Vinyl Bromide
12	1-Pentene	65	Freon-11
13	n-Pentane	66	1,1-Dichloroethene
14	Isoprene	67	Methylene-chloride
15	Trans-2-pentene	68	Allyl Chloride
16	Cis-2-pentene	69	Freon-113
17	2,2-Dimethyl-butane	70	Trans-1,2-Dichloroethene
18	Cyclopentane	71	1,1-Dichloroethane
19	2,3-Dimethylbutane	72	Cis-1,2-dichloroethylene
20	2-Methylpentane	73	Chloroform
21	3-Methylpentane	74	1,2-Dichloroethane
22	1-Hexene	75	1,1,1-Trichloroethane
23	n-Hexane	76	Carbon Tetrachloride
24	Methyl-cyclopentane	77	1,2-Dichloropropane
25	2,4-Dimethylpentane	78	Bromodichloromethane
26	Benzene	79	Trichloroethylene
27	Cyclohexane	80	Cis-1,3-dichloropropene
28	2-Methyl-hexane	81	Trans-1,3-dichloropropene
29	2,3-Dimethyl-pentane	82	1,1,2-Trichloroethane
30	3-Methyl-hexane	83	Dibromochloromethane
31	2,2,4-Trimethyl-pentane	84	1,2-Dibromoethane
32	n-Heptane	85	Tetrachloroethylene
33	Methyl-cyclohexane	86	Chlorobenzene
34	2,3,4-Trimethyl-pentane	87	Bromoform
35	Toluene	88	1,1,2,2-Tetrachloroethane
36	2-Methyl-heptane	89	1,3-Dichlorobenzene
37	3-Methyl-heptane	90	Benzyl Chloride
38	n-Octane	91	1,4-Dichlorobenzene
39	Ethyl-benzene	92	1,2-Dichlorobenzene
40	m/p-Xylene	93	1,2,4-Trichlorobenzene
41	Styrene	94	Hexachloro-1,3-butadiene

42	o-Xylene	95	Acetone
43	n-Nonane	96	Isoproyl Alcohol
44	Isopropylbenzene	97	Carbon Disulfide
45	n-Propylbenzene	98	Methyl Tert Butyl Ether
46	m-Ethyltoluene	99	Vinyl Acetate
47	p-Ethyltoluene	100	Methyl Ethyl Ketone
48	1,3,5-Trimethyl-benzene	101	Ethyl Acetate
49	o-Ethyltoluene	102	Tetrahydrofuran
50	1,2,4-Trimethylbenzene	103	1,4-Dioxane
51	n-Decane	104	Methyl Isobutyl Ketone
52	1,2,3-Trimethylbenzene	105	Methyl Butyl Ketone
53	m-Diethylbenzene	106	Methyl Methacrylate

Table S2. WRF-Chem model settings

Simulation Region	Siping City
Simulation Period	June 11–18, 2021
Simulation Grid Center Coordinates	43.5°N，124.5°E
Horizontal Resolution	6 km × 6 km
Number of Horizontal Grids	150 × 150
Model Vertical Layers	35 layers, with the first layer at approximately 30 meters, and the top layer at approximately 14 km
Microphysical Parameterization Scheme	Morrison Scheme(Morrison et al., 2009)
Boundary Layer Parameterization Scheme	MYJ TKE Parameterization Scheme(Janjić, 1990)
Surface Parameterization Scheme	MYJ Scheme(Janjić, 1990)
Land Surface Process Parameterization Scheme	Integrated Noah Parameterization Scheme (Chen and Dudhia, 2001)
Longwave Radiation Scheme	Goddard Longwave Radiation Scheme(Chou et al., 2001)
Shortwave Radiation Scheme	Goddard Shortwave Radiation Scheme(Chou and Suarez, 1999)
Meteorological Boundary and Initial Conditions	NCEP 1° × 1° Reanalysis Data
Chemical Field Initial and Boundary Conditions	MOZART 6-hour Output Data(Horowitz et al., 2003)
Anthropogenic Emission Inventory	Siping City Anthropogenic Emission Inventory / MEIC Inventory
Biogenic Emission Inventory	Online Calculation from MEGAN Model(Guenther et al., 2006)

Table S3. Sensitivity experiment design for quantifying the contributions of local emissions and regional transport to O_3.

Experiment	Anthropogenic emissions
Baseline simulation (O_3-f_{all})	All anthropogenic emissions included
Sensitivity simulation 1 (O_3-f_{bkgd})	All anthropogenic emissions excluded
Sensitivity simulation 2 (O_3-f_{in})	Only anthropogenic emissions from Siping included
Sensitivity simulation 3 (O_3-f_{out})	Anthropogenic emissions from Siping excluded

Table S4. Sensitivity experiment design for major emission sources affecting O_3.

Experiment	Anthropogenic emissions
Sensitivity simulation 1 (O_3-find)	Industrial emissions excluded
Sensitivity simulation 2 (O_3-fpow)	Power plant emissions excluded
Sensitivity simulation 3 (O_3-fres)	Residential emissions excluded
Sensitivity simulation 4 (O_3-ftra)	Transportation emissions excluded
Sensitivity simulation 5 (O_3-fagr)	Agricultural emissions excluded
Sensitivity simulation 6 (O_3-fbio)	Biogenic emissions excluded

Table S5. Mean concentrations and chemical composition of ambient VOCs in Siping during 2021-2022.

	Concentration (ppbv)	% in group
Alkyne	1.02	2.40%
Alkene	4.50	10.63%
Alkane	15.65	36.98%
Aromatics	2.80	6.61%
Halocarbons	5.04	11.91%
OVOC	13.32	31.48%
TVOC	42.33	100%

Table S6. Concentration characteristics of ambient VOC species in Siping during 2021-2022.

VOCs	Concentration	VOCs	Concentration	VOCs	Concentration
Acetylene	1.02	3-Methylheptane	0.10	1,1-Dichloroethane	0.01
Ethene	1.38	n-Octane	0.08	cis-1,2-Dichloroethene	0.01
Propene	0.62	n-Nonane	0.02	Chloroform	0.39
1-Butene	0.93	n-Decane	0.01	1,2-Dichloroethane	0.40
trans-2-Butene	2.42	n-Undecane	0.00	1,1,1-Trichloroethane	0.00
cis-2-Butene	2.01	n-Dodecane	0.00	Carbon tetrachloride	0.21
Isoprene	0.60	Benzene	0.75	1,2-Dichloropropane	0.18
trans-2-Pentene	3.09	Toluene	1.52	Bromodichloromethane	0.00
1-Pentene	0.74	Ethylbenzene	0.23	Trichloroethene	0.04
cis-2-Pentene	1.33	m,p-Xylene	0.56	cis-1,3-Dichloropropene	0.02
1-Hexene	0.42	Styrene	0.18	trans-1,3-Dichloropropene	0.05
1,3-Butadiene	0.08	o-Xylene	0.19	1,1,2-Trichloroethane	0.02
Ethane	2.52	Isopropylbenzene	0.01	Dibromochloromethane	0.00
Propane	4.88	n-Propylbenzene	0.02	1,2-Dibromoethane	0.03
Isobutane	9.62	m-Ethyltoluene	0.04	Tetrachloroethene	0.57
n-Butane	7.38	p-Ethyltoluene	0.02	Chlorobenzene	0.03
Isopentane	29.14	1,3,5-Trimethylbenzene	0.01	Bromoform	0.00
n-Pentane	10.80	o-Ethyltoluene	0.01	1,1,2,2-Tetrachloroethane	0.08
2,2-Dimethylbutane	0.03	1,2,4-Trimethylbenzene	0.05	1,3-Dichlorobenzene	0.01
Cyclopentane	0.34	1,2,3-Trimethylbenzene	0.01	Benzyl chloride	0.01
2,3-Dimethylbutane	0.67	m-Diethylbenzene	0.00	1,4-Dichlorobenzene	0.02
2-Methylpentane	2.84	p-Diethylbenzene	0.00	1,2-Dichlorobenzene	0.01
3-Methylpentane	2.40	CFC-12	0.54	1,2,4-Trichlorobenzene	0.00
n-Hexane	0.71	Chloromethane	0.80	Hexachloro-1,3-butadiene	0.04
Methylcyclopentane	0.82	CFC-114	0.02	Acetone	11.52
2,4-Dimethylpentane	0.22	Vinyl chloride	0.01	Isopropanol	0.78
Cyclohexane	0.09	Bromomethane	0.01	Methyl tert-butyl ether	0.04
2-Methylhexane	0.58	Chloroethane	0.04	Vinyl acetate	0.63
2,3-Dimethylpentane	0.17	Vinyl bromide	0.00	Methyl ethyl ketone	1.88
3-Methylhexane	0.69	CFC-11	0.25	Ethyl acetate	0.66
2,2,4-Trimethylpentane	0.84	1,1-Dichloroethene	0.00	Tetrahydrofuran	0.11
n-Heptane	0.15	Dichloromethane	1.63	1,4-Dioxane	0.04
Methylcyclohexane	0.14	Allyl chloride	0.00	Methyl isobutyl ketone	0.05

2,3,4-Trimethylpentane	0.50	CFC-113	0.08	Methyl butyl ketone	0.15
2-Methylheptane	0.13	trans-1,2-Dichloroethene	0.02	Methyl methacrylate	0.61

Table S7. Top 15 VOC species in ambient air in Siping during 2021-2022 (ppbv).

2021	Mean concentration	2022	Mean concentration
Isopentane	6.94	Isopentane	49.86
Acetone	4.89	n-Pentane	18.19
Isobutane	3.66	Acetone	17.71
Propane	3.11	Isobutane	15.19
n-Pentane	2.87	n-Butane	13.15
Ethane	2.61	Propane	6.52
Ethene	2.01	trans-2-Pentene	5.92
n-Butane	1.20	2-Methylpentane	5.35
Acetylene	1.15	trans-2-Butene	4.63
Benzene	0.91	3-Methylpentane	4.53
Toluene	0.80	cis-2-Butene	3.85
Methyl ethyl ketone	0.64	Methyl ethyl ketone	3.04
Propene	0.61	Dichloromethane	2.70
Chloromethane	0.56	cis-2-Pentene	2.55
CFC-12	0.55	Ethane	2.43

Table S8. Top 10 VOC species contributing to OFP by month in Siping during 2021-2022.

2021-7	OFP	2021-8	OFP	2021-9	OFP	2022-6	OFP	2022-7	OFP
Isopentane	26.71	Ethene	8.47	Ethene	23.40	Isopentane	134.09	Isopentane	25.29
Ethene	15.88	Propene	2.66	Propene	8.37	trans-2-Pentene	129.01	Isoprene	13.28
Isobutane	9.44	Isoprene	2.01	Isopentane	5.18	trans-2-Butene	114.50	Acetone	13.28
n-Pentane	8.13	Acetone	1.79	Toluene	5.15	cis-2-Butene	95.14	Propene	7.66
Propene	7.76	Isobutane	1.47	Isobutane	3.83	cis-2-Pentene	55.71	Isobutane	6.95
Acetone	3.47	Isopentane	1.08	Acetone	3.44	n-Pentane	44.92	Ethene	6.26
n-Butane	2.47	Propane	0.92	m,p-Xylene	3.10	Isobutane	35.53	1-Butene	3.18
Isoprene	1.98	Toluene	0.64	1-Butene	2.40	n-Butane	32.08	Styrene	1.98
Propane	1.62	1-Butene	0.60	o-Xylene	2.25	1-Pentene	20.36	o-Xylene	1.79
1-Butene	1.49	Ethane	0.50	Propane	2.22	2-Methylpentane	19.74	n-Pentane	1.59

Table S9. Top 10 VOC species contributing to OFP during the morning, afternoon, and evening in Siping during 2021-2022.

Morning	**OFP**	**Afternoon**	**OFP**	**Evening**	**OFP**
Isopentane	35.04	Isopentane	20.24	trans-2-Pentene	75.99
Isobutane	15.56	Ethene	6.81	trans-2-Butene	65.59
n-Pentane	14.39	Acetone	6.44	Isopentane	65.36
Ethene	8.52	Isobutane	5.92	cis-2-Butene	55.66
n-Butane	7.16	n-Pentane	4.08	cis-2-Pentene	33.36
Acetone	6.48	Isoprene	3.27	Ethene	15.36
Propene	5.47	Propene	2.85	n-Pentane	15.21
Isoprene	5.41	trans-2-Butene	2.78	Isobutane	13.45
Toluene	4.24	trans-2-Pentene	2.14	n-Butane	13.36
trans-2-Butene	4.23	n-Butane	2.07	1-Pentene	12.83

Table S10. Contributions of local emissions and regional transport to MDA8 O_3 concentrations in Siping during the simulation period.

	Concentration (μg/m^3)	Contribution (%)
Baseline simulation	155.04	/
Background concentration	88.79	57.27
Local emissions	15.71	10.13
Regional transport	49.89	32.18
Interaction	0.65	0.42

Table S11. Emission reduction scenarios for transportation and industrial sources in Siping.

Total emission reduction (%)	Transportation emissions (VOC/NO_x)	Industry 1: Industrial processes (VOC/ NO_x)	Industry 2: Fossil fuel combustion (VOC/ NO_x)
20%	2.5%/10.3%	2.5%/2.6%	0.7%/5.2%
50%	6.2%/25.7%	6.3%/6.4%	1.7%/13.1%
100%	10.0%/51.3%	12.6%/12.9%	3.4%/26.2%

References

Binkowski, F. S. and Roselle, S. J.: Models-3 Community Multiscale Air Quality (CMAQ) model aerosol component 1. Model description, Journal of Geophysical Research: Atmospheres, 108, https://doi.org/10.1029/2001JD001409, 2003.

Chen, F. and Dudhia, J.: Coupling an Advanced Land Surface–Hydrology Model with the Penn State–NCAR MM5 Modeling System. Part I: Model Implementation and Sensitivity, Monthly Weather Review, 129, 569-585, https://doi.org/10.1175/1520-0493(2001)129<0569:CAALSH>2.0.CO;2, 2001.

Chou, M. and Suarez, M. J.: An efficient thermal infrared radiation parameterization for use in general circulation models, Climate and Radiation Branch, Laboratory for Atmospheres NASAGoddard Space Flight Center Greenbelt MD 20771, 1994.

Chou, M. and Suarez, M. J.: A Solar Radiation Parameterization Atmospheric Studies, National Aeronautics and Space Administration, Goddard Space Flight Center, Greenbelt, Maryland, 1999.

Chou, M., Suarez, M. J., Liang, X., and Yan, M. M. H.: A Thermal Infrared Radiation Parameterization for Atmospheric Studies, National Aeronautics and Space Administration, Goddard Space Flight Center, Greenbelt, Maryland, 2001.

Frischmon, C. and Hannigan, M.: VOC source apportionment: How monitoring characteristics influence positive matrix factorization (PMF) solutions, Atmospheric Environment: X, 21, 100230, https://doi.org/10.1016/j.aeaoa.2023.100230, 2024.

Ginoux, P., Chin, M., Tegen, I., Prospero, J. M., Holben, B., Dubovik, O., and Lin, S.-J.: Sources and distributions of dust aerosols simulated with the GOCART model, Journal of Geophysical Research: Atmospheres, 106, 20255-20273, https://doi.org/10.1029/2000JD000053, 2001.

Grell, G. A., Peckham, S. E., Schmitz, R., McKeen, S. A., Frost, G., Skamarock, W. C., and Eder, B.: Fully coupled "online" chemistry within the WRF model, Atmospheric Environment, 39, 6957-6975, https://doi.org/10.1016/j.atmosenv.2005.04.027, 2005.

Guenther, A., Karl, T., Harley, P., Wiedinmyer, C., Palmer, P. I., and Geron, C.: Estimates of global terrestrial isoprene emissions using MEGAN (Model of Emissions of Gases and Aerosols from Nature), Atmos. Chem. Phys., 6, 3181-3210, 10.5194/acp-6-3181-2006, 2006.

Horowitz, L. W., Walters, S., Mauzerall, D. L., Emmons, L. K., Rasch, P. J., Granier, C., Tie, X., Lamarque, J.-F., Schultz, M. G., Tyndall, G. S., Orlando, J. J., and Brasseur, G. P.: A global simulation of tropospheric ozone and related tracers: Description and evaluation of MOZART, version 2, Journal of Geophysical Research: Atmospheres, 108, https://doi.org/10.1029/2002JD002853, 2003.

Janjić, Z. I.: The Step-Mountain Coordinate: Physical Package, Monthly Weather Review, 118, 1429-1443, https://doi.org/10.1175/1520-0493(1990)118<1429:TSMCPP>2.0.CO;2, 1990.

Li, N., He, Q., Tie, X., Cao, J., Liu, S., Wang, Q., Li, G., Huang, R., and Zhang, Q.: Quantifying sources of elemental carbon over the Guanzhong Basin of China: A consistent network of measurements and WRF-Chem modeling, Environmental Pollution, 214, 86-93, https://doi.org/10.1016/j.envpol.2016.03.046, 2016.

Li, R., Xia, Z., You, B., Shi, B., and Fu, J.: Volatile Organic Compound Emission Inventory for Pesticide Spraying in an Agricultural City of Northeast China: Real-Time Monitoring and Method Optimization, Agriculture, 14, 1223, 2024.

Liang, X., Sun, X., Xu, J., and Ye, D.: Improved emissions inventory and VOCs speciation for industrial OFP estimation in China, Science of The Total

Environment, 745, 140838, https://doi.org/10.1016/j.scitotenv.2020.140838, 2020.
Lyu, C., Capps, S. L., Kurashima, K., Henze, D. K., Pierce, G., Hakami, A., Zhao, S., Resler, J., Carmichael, G. R., Sandu, A., Russell, A. G., Chai, T., and Milford, J.: Evaluating oil and gas contributions to ambient nonmethane hydrocarbon mixing ratios and ozone-related metrics in the Colorado Front Range, Atmospheric Environment, 246, 118113, https://doi.org/10.1016/j.atmosenv.2020.118113, 2021.
Man, H., Liu, H., Niu, H., Wang, K., Deng, F., Wang, X., Xiao, Q., and Hao, J.: VOCs evaporative emissions from vehicles in China: Species characteristics of different emission processes, Environmental Science and Ecotechnology, 1, 100002, https://doi.org/10.1016/j.ese.2019.100002, 2020.
Mellor, G. L. and Yamada, T.: Development of a turbulence closure model for geophysical fluid problems, Reviews of Geophysics, 20, 851-875, https://doi.org/10.1029/RG020i004p00851, 1982.
Monin, A. S. and Obukhov, A. M.: Basic laws of turbulent mixing in the surface layer of the atmosphere, Tr. Akad. Nauk SSSR Geophiz. Inst., 24(151):163-187, 1954.
Morrison, H., Thompson, G., and Tatarskii, V.: Impact of Cloud Microphysics on the Development of Trailing Stratiform Precipitation in a Simulated Squall Line: Comparison of One- and Two-Moment Schemes, Monthly Weather Review, 137, 991-1007, https://doi.org/10.1175/2008MWR2556.1, 2009.
Sha, Q. e., Zhu, M., Huang, H., Wang, Y., Huang, Z., Zhang, X., Tang, M., Lu, M., Chen, C., Shi, B., Chen, Z., Wu, L., Zhong, Z., Li, C., Xu, Y., Yu, F., Jia, G., Liao, S., Cui, X., Liu, J., and Zheng, J.: A newly integrated dataset of volatile organic compounds (VOCs) source profiles and implications for the future development of VOCs profiles in China, Science of The Total Environment, 793, 148348, https://doi.org/10.1016/j.scitotenv.2021.148348, 2021.
Sun, L., Zhong, C., Peng, J., Wang, T., Wu, L., Liu, Y., Sun, S., Li, Y., Chen, Q., Song, P., and Mao, H.: Refueling emission of volatile organic compounds from China 6 gasoline vehicles, Science of The Total Environment, 789, 147883, https://doi.org/10.1016/j.scitotenv.2021.147883, 2021.
Vestenius, M., Hopke, P. K., Lehtipalo, K., Petäjä, T., Hakola, H., and Hellén, H.: Assessing volatile organic compound sources in a boreal forest using positive matrix factorization (PMF), Atmospheric Environment, 259, 118503, https://doi.org/10.1016/j.atmosenv.2021.118503, 2021.
Wang, L., Slowik, J. G., Klein, F., Stefenelli, G., Pospisilova, V., Tong, Y., Baltensperger, U., and Prévôt, A. S. H.: Characteristics of oxygenated volatile organic compounds in Zurich, Switzerland: Sources, composition, and implication for secondary aerosol formation, Chemosphere, 368, 143686, https://doi.org/10.1016/j.chemosphere.2024.143686, 2024.
Wang, Z., Zhang, P., Pan, L., Qian, Y., Li, Z., Li, X., Guo, C., Zhu, X., Xie, Y., and Wei, Y.: Ambient Volatile Organic Compound Characterization, Source Apportionment, and Risk Assessment in Three Megacities of China in 2019, 10.3390/toxics11080651, 2023.
Wu, Y., Liu, B., Meng, H., Dai, Q., Shi, L., Song, S., Feng, Y., and Hopke, P. K.: Changes in source apportioned VOCs during high O3 periods using initial VOC-concentration-dispersion normalized PMF, Science of The Total Environment, 896, 165182, https://doi.org/10.1016/j.scitotenv.2023.165182, 2023a.
Wu, Y., Fan, X., Liu, Y., Zhang, J., Wang, H., Sun, L., Fang, T., Mao, H., Hu, J., Wu, L., Peng, J., and Wang, S.: Source apportionment of VOCs based on photochemical loss in summer at a suburban site in Beijing, Atmospheric Environment, 293, 119459, https://doi.org/10.1016/j.atmosenv.2022.119459,

2023b.
Ye, X., Yang, J., Chen, Z., Liu, G., Sun, J., Jiang, Q., Huang, X., Gao, Y., Niu, X., Xu, H., Li, G., and Shen, Z.: Triangulating residential biomass burning impacts on PM2.5 via PMF, satellite observation-based emission inventory, and WRF-Chem, Environment International, 201, 109580, https://doi.org/10.1016/j.envint.2025.109580, 2025.
Zhou, M., Jiang, W., Gao, W., Zhou, B., and Liao, X.: A high spatiotemporal resolution anthropogenic VOC emission inventory for Qingdao City in 2016 and its ozone formation potential analysis, Process Safety and Environmental Protection, 139, 147-160, https://doi.org/10.1016/j.psep.2020.03.040, 2020.
Zhu, J., Xia, S., Niu, H., Xu, J., Wang, Y., Yu, X., Huang, L., Zhang, K., Wang, Y., Zeng, L., Li, Q., and Li, L.: Volatile organic compounds from typical industries in North China Plain: emissions, air pollution contribution, health risks, and policy implications, Environment International, 202, 109673, https://doi.org/10.1016/j.envint.2025.109673, 2025.
Zi, T., Wang, P., Liu, B., Zhou, Y., Shen, X. e., Zhang, L., Lu, Y., Feng, Q., Yang, Y., and Lang, J.: Evaporative emission characteristics of VOCs from in-use light-duty gasoline vehicles, Atmospheric Environment, 312, 120024, https://doi.org/10.1016/j.atmosenv.2023.120024, 2023.